Nigerian Journal of Science and Environment 2024 Volume 22 (1) 180 – 193 ISSN: 1119 – 9008
https://doi.org/10.61448/njse2212414

ASSESSMENT OF SUBSOIL CORROSIVITY USING GEOELECTRIC LAYER PARAMETERS AT ILERE COMMUNITY NEAR AKURE, SOUTHWESTERN NIGERIA

Adeyemo Igbagbo A. [1*], Gade Adefolarinwa E. [1], Olaniyan Opeyemi A. [1] and Aruwaji Success I.

[1]*Department of Applied Geophysics, Federal University of Technology, Akure, Nigeria*

**Corresponding author's e-mail: iaadeyemo@futa.edu.ng*

ABSTRACT
Fifty-nine (59) vertical electrical sounding (VES) data were acquired within Ilere community, near Akure southwestern Nigeria to characterize the area into different corrosivity zones at different depth surfaces. The acquired field data were interpreted using manual curve matching technique and the initial layer parameters (resistivity and thickness) were iterated to produce the final geoelectric parameters (resistivity and thickness). Since metallic utilities are installed at different depths depending on their purpose, the VES results were presented as table, topsoil and iso-resistivity depths slice maps (0.5, 0.75, 1.0 and 3.0 m) in order to make the research work relevant for different uses. The 0.5 m depth slice isoresistivity map shows that about 75% of this depth surface are of higher resistivity (above 201 Ωm) suggesting negligible corrosivity. The 0.75 m depth slice isoresistivity map indicated that about 70% of this depth surface are of higher resistivity (above 201 Ωm) suggesting negligible corrosivity. Likewise, the 1.0 m depth slice isoresistivity map shows that about 60% of this depth surface are of higher resistivity (above 201 Ωm) suggesting negligible corrosivity. Finally, the 3.0 m depth slice isoresistivity map shows that about 35% of this depth surface are of higher resistivity (above 201 Ωm) suggesting negligible corrosivity. There is a reduction in the percentage of the portion delineated to be of negligible corrosivity in each depth slices of the study area as we move deeper into the subsurface.

Keywords: Subsoil, corrosivity, assessment, geoelectric parameters

INTRODUCTION

Soil corrosion is a geologic hazard that affects buried metals and concrete that is in direct contact with soil or bedrock (Idornigie *et al.*, 2006; Guma *et al.*, 2015). Soil corrosion is the deterioration of metal or other materials brought about by chemical, mechanical, and biological action by soil environment. Corrosion exists in virtually all materials, but is mostly often associated with metals. Corrosion is the gradual chemical attack and degradation that results in the conversion of metallic materials into oxides, salts or other compounds. Materials such as metals and its alloys that have undergone corrosion lose their strength, ductility and other mechanical properties (Najjaran et al., 2004; Hussain and Tarig, 2014). Corrosion attacks are frequently responsible for most materials failures.

Natural gas, crude oil pipelines and metallic water pipes are some of the underground infrastructure reported to have been affected by soil corrosion all around the world. The failure of gas, crude oil pipeline or underground pipe are usually accompanied by high degree of environmental, human and economic consequences (Akintunde and Ozebo, 2022). The major cause of the deterioration of underground pipeline is the soil and moisture (Rim-rukch, 2006; Hussain and Tarig, 2014).

Soil corrosion is usually caused by a number of factors such as; moisture, pH, redox potential, subsoils' microbes and soil type (Palmer, 1989; Picozzi et al., 1993; Rim-rukch, 2006; Hussain and Tarig, 2014). The study of different soil types showed that there is a link between the soil properties and its corrosiveness (Palmer, 1989). Soil resistivity is the most used indicator of soil corrosivity (Braford, 2000). Consequently, understanding the resistivity of soil's composition is a key factor for monitoring or predicting the level of soil corrosion. Electrical resistivity method can be use in detecting areas of high corrosion (hot spots) along the buried underground metals. The corrosivity of soils is nearly inversely proportional to their resistivity: that is low resistivity, means a high probability of corrosion (Andrew *et al*., 2005). Resistivity and spontaneous potential (SP) are two electrical properties of rocks commonly measured. Taken separately or together, these two measurements provide a good indication of some important lithologic distinctions in the subsurface (Bayowa and Olayiwola, 2015).

Electrical resistivity method have been successfully used in many corrosivity investigation works (Bayowa and Adigun, 2012; Adeoti et al., 2013; Hussain and Tarig, 2014; Alagbe, 2018; Adeyemo et al., 2018; Adeyemo et al., 2019; Akintunde and Ozebo, 2022; Eyankware and Umaya, 2022). It has also been reported that soil resistivity is the best criterion for estimating the corrosion of a given soil in the laboratory, where the vital parameter of moisture can be controlled (Dayal et al., 1988).

Idornigie et al. (2006) on the basis of resistivity contrast classified the subsoil of Akungba-Akoko, Ondo State, Nigeria into four corrosivity zones; very strongly corrosive (less than 10 ohm- m), moderately corrosive (10 - 60 Ωm), slightly corrosive (60 - 180 Ωm) and non- corrosive (180 Ωm and above).

Guma et al. (2015) also undertook a search on soil corrosivity level of Kaduna metropolitan area using electrical resistivity method. In terms of soil corrosivity rating, the study area was described as mildly corrosive on the average and generally varies downwards from aggressive at depths of less than about 0.5 m to slightly corrosive around 4.5 m depth.

Adeyemo et al. (2018) carried out an assessment of Subsurface Corrosivity in Ondo State Industrial Layout, Akure, Southwestern Nigeria using depth slices iso-resistivity. The area was categorized into five corrosive zones based on their range of resistivity values; very strongly corrosive (below 60 Ωm), strongly corrosive (60 - 150 Ωm), moderately corrosive (150 - 250 Ωm), slightly corrosive (250 - 350 Ωm), and non-corrosive (above 350 Ωm). This characterization was done at three different depth slices (1.0, 2.0 and 3.0 m). Comparison of the three depth slice maps indicated that corrosivity increase with depth in the study area within the shallow subsurface.

Problem Definition

Ilere area is a fast growing community where many residential and industrial buildings are springing up. Among such industrial buildings are filling stations where underground storage tanks are usually installed. Corrosion of such underground storage tanks may cause leakage and rupturing of such tanks resulting in serious environmental pollution and financial losses. It is therefore important to characterize the town into different corrosivity zones in order to recommend safer areas within the town where underground storage tanks can be installed safely with minimum risk of corrosion

Study Area

Ilere community is located about 2 km from Akure in northwest direction, Southwestern Nigeria (Figure 1). The study area "Ilere" is located along Ijare road (Figure 1) and the area falls within coordinates 738567 - 739035 m (Eastings) and 806719 - 812694 m (Northings) on Universal Traverse Mercatum system. It is a well built-up area and is accessible through a major tarred road, few untarred roads and many footpaths. The area is moderately to highly undulating with surface elevation ranging from 354 - 398 m above sea level (Figure 2). The climate is hot and humid, influenced by the rain forest of the southwestern Nigeria. The rainy season lasts from April to October, with rainfall of about 152 mm per year. The average temperature is about 27^{0}C during harmattan (December - February) and 32^{0}C in March with mean annual relative humidity of about 80% (Iloeje, 1980; Adeyemo et *al.*, 2023).

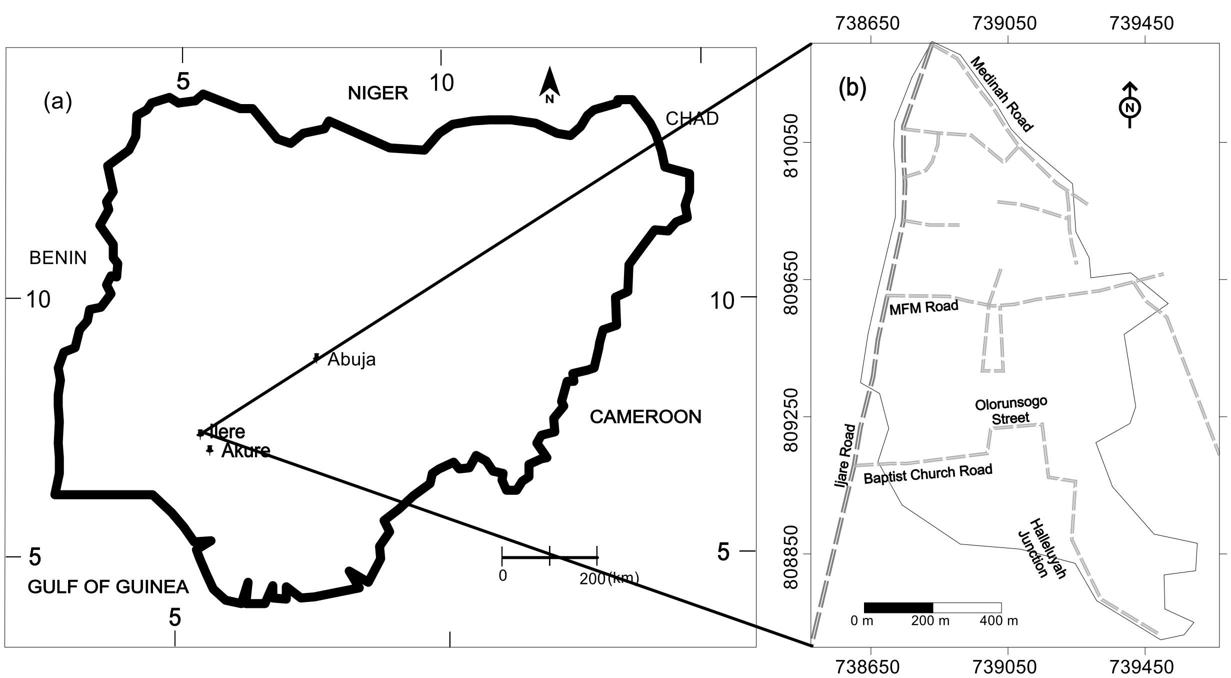

Figure 1$_{(a-b)}$. (a) Sketch map of Nigeria showing relative position of Akure and Ilere (After Adeyemo et al., 2023), (b) Layout map of Ilere town

Nigerian Journal of Science and Environment 2024 Volume 22 (1) 180 – 193 ISSN: 1119 – 9008
https://doi.org/10.61448/njse2212414

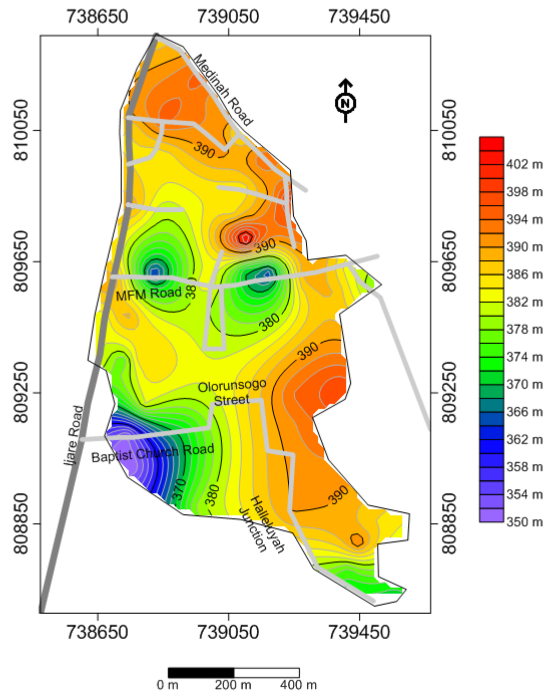

Figure 2. Topographic map of Ilere town

Geology of the Area

Two rock units; migmatite-gneiss and older granite underlie the study area (Figure 3) (Mogaji et al., 2022). The migmatite-gneiss occurs as series of low-lying rubbles and folded-like veins and has segregation of light colored granitic composition, while the older granite occurs either as charnockites or porphyritic granite.

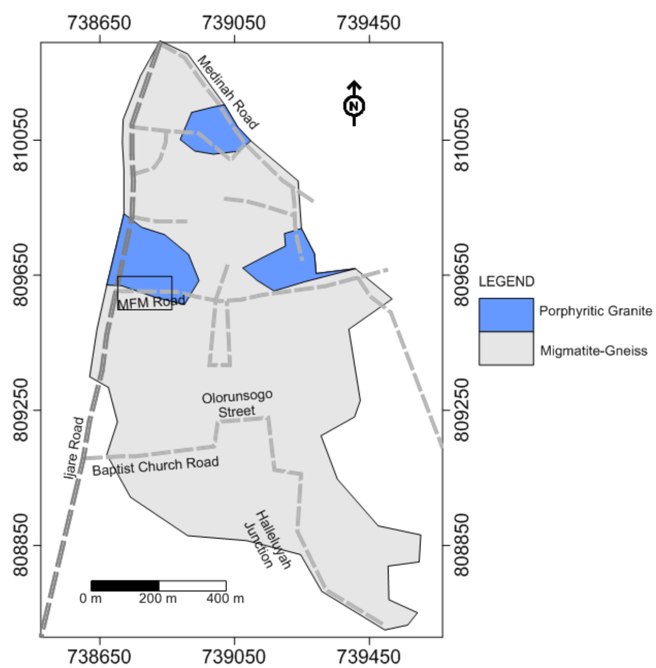

Figure 3. Simplified geologic map of Ilere town

MATERIALS AND METHODS

The Omega Earth Resistivity meter was used for the data acquisition. Vertical electrical sounding (VES) data were acquired using Schlumberger electrode configuration (Figure 4) with maximum half-current electrode separation (AB/2) of 65 - 100 m. A total fifty-nine (59) VES data were acquired in the area (Figure 5). The VES was measured with respect to a fixed center, to acquire this; potential differences are measure at different positions of the current electrode with respect to a fixed center, which is the station position. As the electrode separation is increasing, the potential difference values starts dropping. This reducing potential difference is compensated by increasing the potential electrodes separation. The apparent resistivity values of the each successive layers are determined from the following Schlumberger configuration equations (Equations 1- 3).

Thus, $\rho_{Schlumberger} = 2\pi R\left[\frac{L^2 - l^2}{4l}\right]$ (1)

When L>>>l i.e. $L^2 - l^2 \approx L^2$

Such that,

$$\rho_a = \frac{\pi R L^2}{2l} \quad (2)$$

Equation 2 can also be written as,

$$\rho_a = \frac{\pi R \left(^{AB}/_2\right)^2}{MN} \quad (3)$$

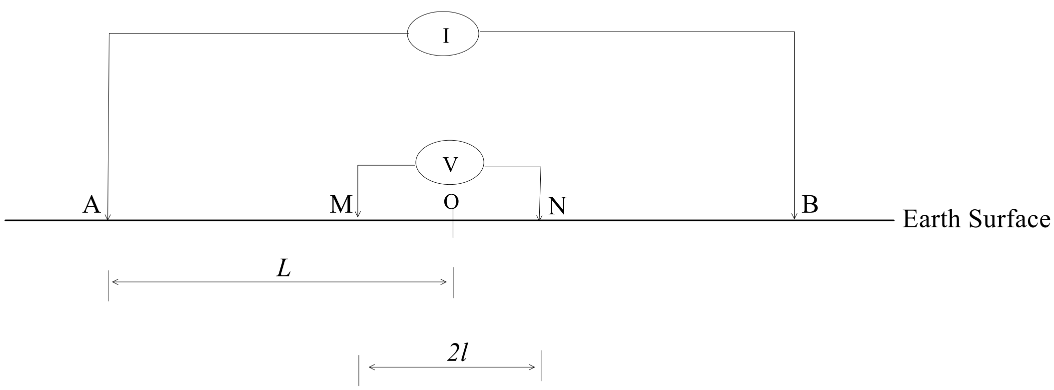

Figure 4. Schlumberger Electrode Configuration (Source: Zohdy *et. al.*, 1974).

Where,

A is the position of current electrode 1, which is the source

B is the position of current electrode 2, which is the sink

M and N are the positions of potential electrodes 1 and 2; the two potential terminals

https://doi.org/10.61448/njse2212414

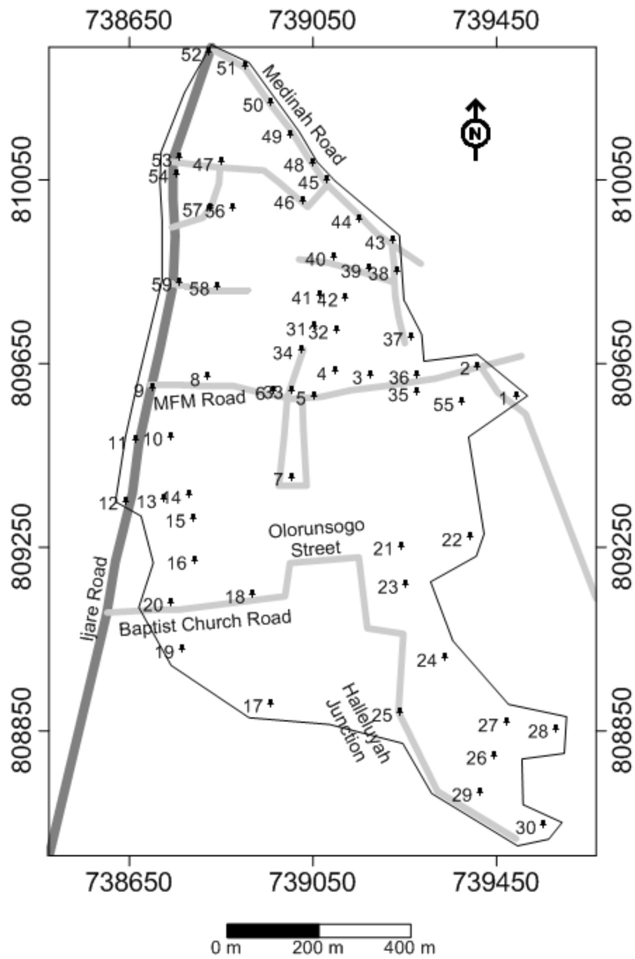

Figure 5. Sketch map of Ilere showing VES points

The apparent resistivity (ρ_a) values were subsequently plotted on a bi-log paper as VES curves and then interpreted using conventional manual curve matching technique (Keller and Frischknecht, 1966 and Koefeod, 1979). This exercise yielded the initial layer parameters (resistivity and thickness). The initial layer parameters were subsequently iterated using window Resist, a 1-D forward modelling software (Vander Velpen, 2004). The final iterated results were presented in table 1. The VES results were also presented as maps of topsoil resistivity and iso-resistivity at different depth slices (0.5, 0.75, 1.0 and 3.0 m). All the resistivity maps of the study area were characterized into different corrosivity zones based on Gopal (2010) classification (Table 2).

RESULTS AND DISCUSSION

The VES results delineated lithologic sequences underlain by three to four geo-electric layers. The A, H, K, Q, AK, HA, KH, HK, KQ, QH, are the ten different sounding curve types delineated in the area (Table 1). The KH and H curve are the predominant type in the area with percentage occurrence of 26% each, the A curve has 18% occurrence, the K and Q curve has 5% occurrence each, the HK curve has 10% occurrence, the HA curve has 5.2% occurrence, the QH, AK and KQ curves are the least with 1.6% occurrence each.

The resistivity of the top soil, weathered layer, partly weathered layer and weathered bedrock/fresh bedrock varies from 26 - 1226 Ωm, 29 - 2478 Ωm, 22 - 5597 Ωm and 146 - 7325 Ωm respectively, while their thickness varies respectively from 0.2 - 9 m, 0.1 - 44 m and 0.5 - 22.7 m in the three upper layers.

Table 1: The VES Summary Results

VES NO	Easting (m)	Northing (m)	Resistivity $\rho_1/\rho_2/\ldots/\rho_n$ (Ωm)	Thickness $h_1/h_2/\ldots/h_n$ (m)	Curve Type
1	739493	809573	40/1083/108/4023	1/1.5/7.8	KH
2	739409	809638	31/402/4234	3.9/4	A
3	739175	809618	59/101/2070	0.9/8	A
4	739098	809627	201/396/111/4634	2/0.4/3.6	KH
5	739052	809573	69/179/822/7325	4/1/0.6	AA
6	738964	809584	64/101/41/1666	3.7/1/2.6	KH
7	739003	809396	53/522/22/7407	0.4/0.8/3.7	KH
8	738821	809614	205/72/385	2/5.9	H
9	738699	809590	101/270/799/156	1.2/12.1/6.5	AK
10	738740	809484	380/117/567/213	0.6/0.9/6.8	HK
11	738663	809476	201/357/243	0.5/14.4	K
12	738643	809344	86/904/265	2.2/6.9	K
13	738726	809348	281/101/557/199	0.7/0.3/15.2	HK
14	738781	809357	533/324/639/180	0.6/1/9.7	HK
15	738789	809306	188/429/337/169	0.8/0.5/22.7	KQ
16	738792	809214	69/273/43/806	0.3/8.5/0.5	KH
17	738958	808903	48/387/528	0.2/0.7	A
18	738919	809141	244/462/254/440	0.6/1.3/8	KH
19	738765	809021	126/356/146	1.2/44	K
20	738741	809123	78/124/362	2.8/0.3	A
21	739243	809246	75/160/62/1422	0.7/2.2/4	KH
22	739392	809265	114/96/108/915	1.3/0.1/14.2	HA
23	739253	809162	144/944/109/955	0.3/1.5/7.5	KH
24	739338	809002	38/64/1656	0.4/3.9	Q
25	739240	808883	132/603/94/1088	0.2/1.8/7.4	KH
26	739446	808790	56/597/229/925	0.5/0.7/6	KH
27	739471	808861	111/273/5597	2.6/0.6	Q
28	739580	808848	148/1167/965	0.8/5.2	K
29	739414	808709	61/254/16/306	0.4/3.5/1.4	KH
30	739553	808638	153/31/220/1488	1/1.2/1.4	HA
31	739053	809724	420/46/1649	0.7/5.6	H
32	739101	809717	113/64/886	0.9/4	H

33	739003	809586	408/88/2747	0.2/6.9	H
34	739024	809672	91/24/639/4603	0.7/2.8/2.8	HA
35	739275	809581	234/29/1763	0.9/7.4	H
36	739277	809618	146/35/623	0.3/4.6	H
37	739264	809702	98/72/18/1500	2.2/0.2/1.4	QH
38	739232	809845	128/2478/477/648	1.5/0.1/4.2	KH
39	739172	809850	86/449/155/876	0.6/0.7/11	KH
40	739095	809876	298/163/755	1/9.9	Q
41	739065	809792	205/96/1274	0.5/6	H
42	739121	809787	121/130/2617	1.7/7.3	A
43	739225	809912	160/252/1917	5.2/0.2	A
44	739152	809957	50/125/2064	0.3/19.1	A
45	739080	810043	61/155/1615	0.8/11	A
46	739027	809999	218/169/1178	0.6/8.4	H
47	738850	810082	559/178/1040	0.4/15.9	H
48	739048	810081	258/116/597	0.3/5.9	H
49	739000	810143	239/61/151/794	0.7/0.8/10.9	HK
50	738959	810212	1226/228/863	0.5/17.2	H
51	738901	810292	126/33/138/327	2/0.6/0.4	HK
52	738824	810322	135/415/24/1506	0.7/2.3/5.1	HK
53	738760	810092	277/113/745	0.8/2.9	H
54	738753	810057	218/300/1617	9/10.2	Q
55	739374	809559	26/592/230/1224	0.3/0.8/12.1	KH
56	738876	809981	628/31/1599	2.1/2.6	H
57	738827	809983	249/143/906	3.6/15.4	H
58	738842	809812	140/209/1170	1.5/18.8	A
59	738760	809821	140/135/550	1.5/9	H

Table 2: Classification of soil corrosiveness from soil resistivity (Gopal, 2010)

Resistivity (Ωm)	Corrosive Probability
>200	Negligible
100 - 200	Low
50 - 100	High
<50	Very High

Topsoil Resistivity

The topsoil resistivity map (Figure 6) shows resistivity values ranging from 26 - 1226 Ωm across the study area. Very low resistivity values (< 50 Ωm) and low resistivity values (51 - 100 Ωm) which corresponds to very high corrosivity and high corrosivity respectively were observed at the northeastern, southeastern and pockets of places in the southwestern parts of the area. These sections account for about (35%) of the study area. The high resistivity values (151 - 200 Ωm) and higher resistivity values

(201 Ωm and above) which suggests low corrosivity and negligible corrosivity respectively were observed in northwestern and a major segment of the western parts of the area. The area characterized by low corrosivity and negligible corrosivity covered about 30% of the area. The remaining 30% of the study area are of moderate topsoil resistivity (101 - 150 Ωm) corresponding to moderate corrosivity.

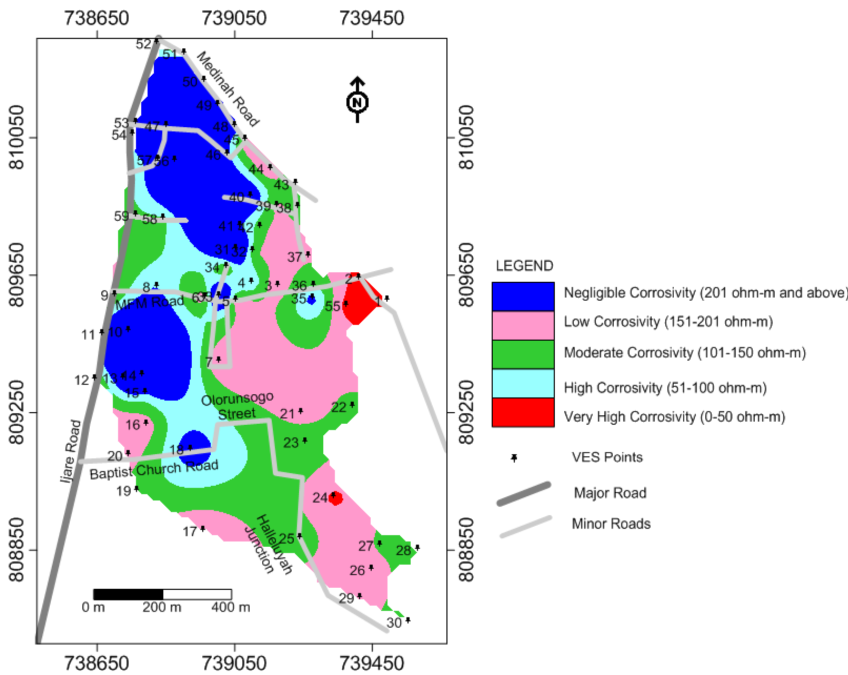

Figure 6. Topsoil resistivity map of the area

Depth-slice Isoresistivity Maps

Subsurface corrosivity studies are better presented as depth slices in order to provide information on targeted depth of interest. Metallic utilities are buried at different depths depending on their purposes. Water pipe lines are buried at about 0.5 m depths, oil-pipe lines are mostly buried at 0.75 - 1.0 m depths, and petrol filling station's storage tanks are buried at about 3.0 m depth. Presenting our results as iso-resistivity depths slice maps will make the research work applicable to different uses.

0.5 m Depth Slice Isoresistivity Map

The 0.5 m depth slice isoresistivity map (Figure 7) shows that about 75% of the depth surface are of higher resistivity (above 201 Ωm) suggesting negligible corrosivity. The remaining 25% of the area are characterized by high resistivity (151 - 200 Ωm) and moderate resistivity (101 - 150 Ωm) which corresponding to low corrosivity and moderate corrosivity. The study shows that, at this depth, buried metallic objects are at a lower risk of corrosion at the northern, southern, and western parts of the study area. Steel water pipelines will last longer at this depth surface of the study area.

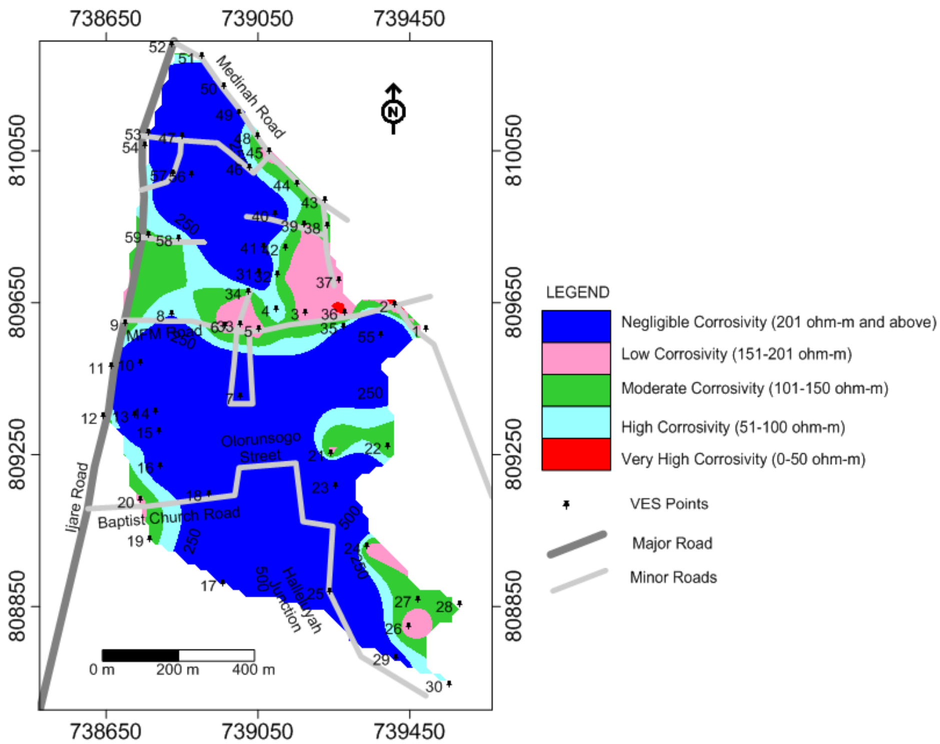

Figure 7. 0.5 m depth slice isoresistivity map

0.75 m Depth Slice Isoresistivity Map

The 0.75 m depth slice isoresistivity map (Figure 8) shows that about 70% of this depth surface are of higher resistivity (above 201 Ωm) suggesting negligible corrosivity. The remaining 25% of the area are characterized by low resistivity (51 - 100 Ωm) and moderate resistivity (101 - 150 Ωm) which corresponding to high corrosivity and moderate corrosivity respectively.

1.0 m Depth Slice Isoresistivity Map

The 1.0 m depth slice isoresistivity map (Figure 9) shows that about 60% of this depth surface are of higher resistivity (above 201 Ωm) suggesting negligible corrosivity especially at the southern and most part of the northern sections of the area. About 35% of the area are characterized by low resistivity (51 - 100 Ωm) and moderate resistivity (101 - 150 Ωm) which corresponding to high corrosivity and moderate corrosivity respectively mainly at the central part of the area. The remaining 5% of this depth surface are characterized by very low resistivity (less than 51 Ωm) and high corrosivity (151 - 201 Ωm) which corresponds to very corrosivity and low corrosivity respectively, this occurs at the central part of the area.

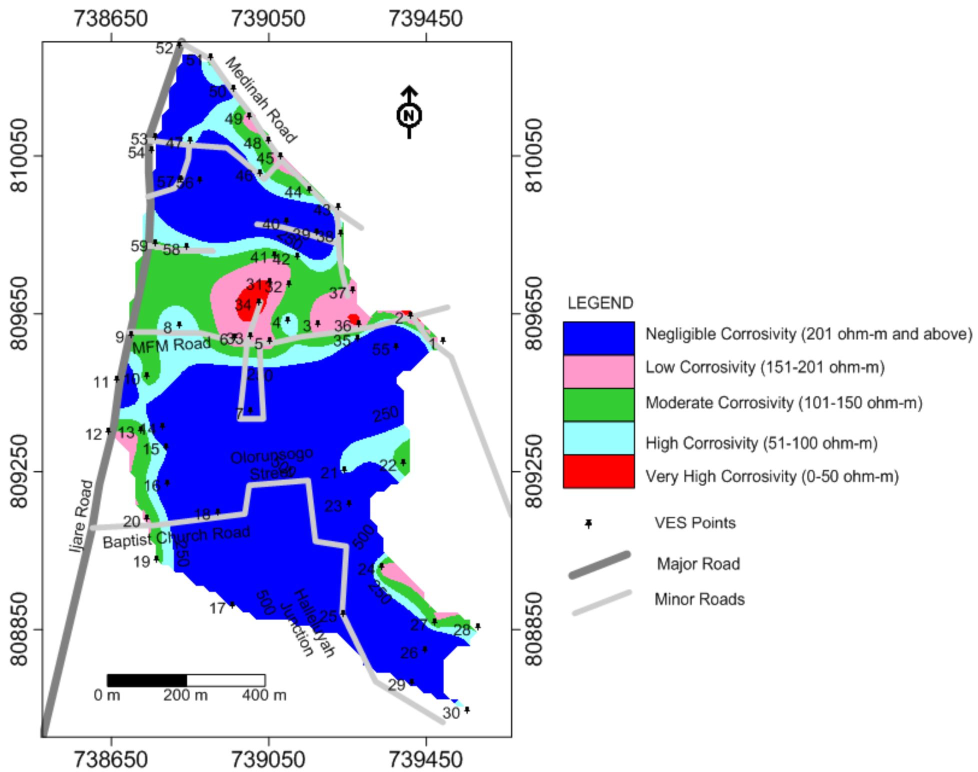

Figure 8. 0.75 m Depth Slice Isoresistivity Map

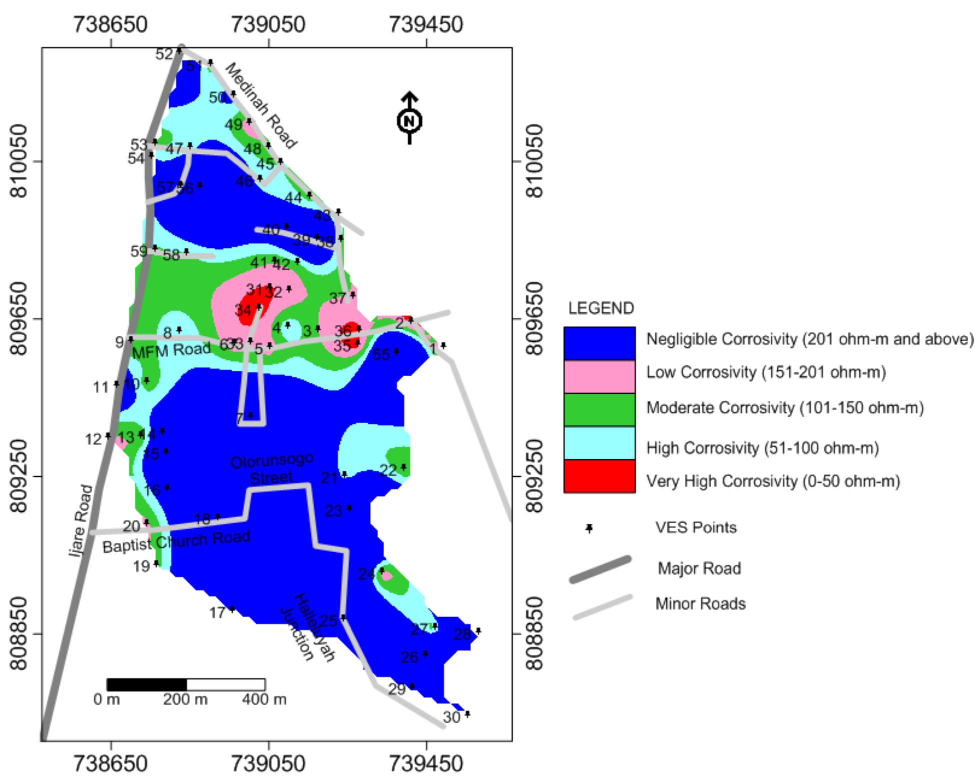

Figure 9. 1.0 m Depth Slice Isoresistivity

Nigerian Journal of Science and Environment 2024 Volume 22 (1) 180 – 193 ISSN: 1119 – 9008
https://doi.org/10.61448/njse2212414

3.0 m Depth Slice Isoresistivity Map

The 3.0 m depth slice isoresistivity map (Figure 10) shows that just about 35% of this depth surface are of higher resistivity (above 201 Ωm) suggesting negligible corrosivity. This is observed at the western and extreme southeastern sections, and pockets of places in the northern section of the area. About 45% of the area are characterized by low resistivity (51 - 100 Ωm) and moderate resistivity (101 - 150 Ωm) which corresponding to high corrosivity and moderate corrosivity respectively mainly at the northern and southeastern parts of the study area. The remaining 20% of this depth surface are characterized by very low resistivity (less than 51 Ωm) and high resistivity (151 - 201 Ωm) which corresponds to very high corrosivity and low corrosivity respectively, this occurs at the central part of the area.

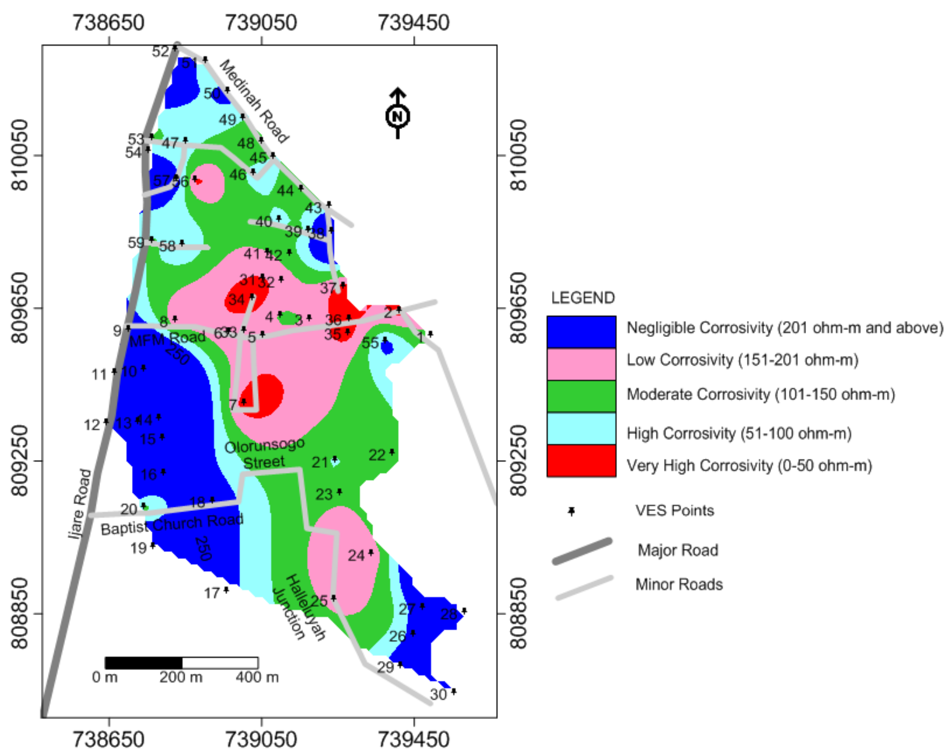

Figure 10. 3.0 m Depth Slice Isoresistivity

CONCLUSION

In order to characterize Ilere community into different corrosivity zones at different depth surfaces, VES technique of electrical resistivity method was adopted for the data acquisition. The VES field data were interpreted using the conventional manual curve matching technique and the resultant layer parameters (resistivity and thickness) were iterated to produce the final geoelectric parameters (resistivity and thickness). The VES results were presented as iso-resistivity depths slice maps in order to make the research outcome relevant to different uses. The 0.5 m, 0.75 m, 1.0 m and 3.0 m depth slice isoresistivity maps shows that about 75%, 70%, 60% and 35% of their respective depth surfaces are of higher resistivity (above 201 Ωm) suggesting negligible corrosivity. This indicated a reduction in the percentage of the portion delineated to be of negligible corrosivity in each depth surfaces as the depth increases. This implies that corrosivity increases with depth in the study area which agrees with subsurface moisture variation.

ACKNOWLEDGEMENT
The authors are grateful to the Department of Applied Geophysics, Federal University of Technology, Akure, Nigeria for allowing the use of Ohmega Earth Resistivity meter. We also grateful to some students of the same Department who assisted in acquiring data for this work.

REFERENCES

Adeoti, L., Ishola, K. S. and Adesanya, O. (2013): Subsurface Investigation Using Electrical Resistivity and Standard Penetration Test as Guide for Gas Pipeline Installation in Lekki Peninsula, Lagos. *European Journal of Geology and Environment (EJGE).* 18, 2791-2804.

Adeyemo, I. A. Olumilola, O. A. and Ibitomi, M. A. (2018): Geoelectrical and geotechnical investigations of subsurface corrosivity in Ondo State Industrial Layout, Akure, Southwestern Nigeria. *Ghana Mining Journal*. 18(1), 20-31. DOI.org/10.4314/gm/v18i1.3.

Adeyemo, I. A., Karounwi, S. A. and Oladeji, J. F. (2019): Geoelectric sounding and soil physico-chemical tests for subsurface layers corrosivity investigations at Ilaramokin, near Akure, Southwestern Nigeria. *IOSR Journal of Applied Geology and Geophysics.* 7(6) Series III, 25-36. DOI: 10.9790/0990-0706032536.

Adeyemo, I. A., Afolayan, A. I., Boluwade, B. S. and Alabi, S. K. (2023): Subsurface geotechnical competence evaluation using geoelectric sounding and direct cone penetrometer test at Plural Garden Estate, Ilaramokin Southwestern Nigeria. *Indonesian Journal of Earth Sciences.* 3(2), 1-11. DOI: 10.52562/injoes.2023.618.

Akintunde, O. A. and Ozebo, V. C. (2022): Integrated approach in evaluating subsurface corrosivity condition along a proposed gas pipe route at Obasanjo Farm, Obada Oko in Ogun State, Nigeria. *Arabian Journal of Geosciences*. 15:1329. https://doi.org/10.1007/s12517-022-10539-y

Alagbe, O. A. (2018): 2D Geoelectrical resistivity imaging for the assessment of subsurface soil corrosivity zones at a proposed filling station site in Akure Southwestern Nigeria. *International Advanced Research Journal in Science, Engineering and Technology*. 5(11), 58-73.

Andrew, E. R., Graham, E. C. B., Sleven, J. D. and Forman. S. (2005): External corrosion and corrosion control of buried water. *American Water Works Association (AWWA) Research Foundation* 159.

Bayowa, O. G. and Adigun O. A. (2012): Evaluation of subsoil corrosivity condition around a sewage pond using the electrical resistivity method. A Case Study from the Basement Complex Terrain of Ile-Ife, Southwestern Nigeria. *Greener Journal of Physical Sciences*, 2(1), 010-015.

Bayowa, O. G., and Olayiwola, F. A. (2015): Electrical resistivity investigation on topsoil thickness, competence and corrosivity to determine soil suitability for building construction. *International Journal of Scientific and Engineering Research*, 6(3), 2073-2084.

Beavers, J. A. and Thompson, N. G. (2006): External Corrosion of Oil and Natural Gas Pipelines. *ASM International Handbook*. 514(13), 1-12.

Braford, L. J. (2000): Electrical resistivity testing. In Nondestructive Testing Handbook, Second Edition: Infrared and

Thermal Testing, *ASM International Handbook*, 7, 309-345.

Dayal, R., Dayal, R., Singh, T. N. and Tewari, R. P. (1988): Studies on corrosion control of underground metallic structures: estimation of corrosion using different soil parameters. *Corrosion Science*, 28(3), 205-219.

Eyankware, M. O. and Umayah, S. O. (2022): 1D modeling of aquifer vulnerability and soil corrosivity within the sedimentary terrain in Southern Nigeria, using resistivity method. *World News of Natural Sciences, An International Scientific Journal*, 41, 33-50.

Gopal, M. (2010): Corrosion potential assessment. The Geology of part of Southwestern Nigeria. *Geological Survey of Nigeria*, 31-87.

Guma, D. K., Aondover, A. P. and Onoja, A. (2015): Soil corrosivity level of Kaduna metropolitan area using electrical resistivity method. *International Journal of Scientific and Engineering Research*, 6(2), 1408-1419.

Hussain, T. and Tarig, A. (2014): Study on corrosion rate of carbon steel in different soils. *Arabian Journal for Science and Engineering*, 39(12), 8165-8172.

Idornigie, A. I., Ehirim, N. C. and Anyiam, O. S. (2006): Determination of subsoil corrosivity zones in Akungba-Akoko area, Nigeria using electrical resistivity method. *Journal of Mining and Geology*, 42(2), 115-124.

Iloeje, N. P. (1980): A new Geography of Nigeria (New Revised Edition). London, UK; Longman Group.

Keller, G. V. and Frischknecht F. C. (1966): Electrical Methods in Geophysical Prospecting. *Pergamon Press, Oxford*.

Mogaji, K. A., Atenidegbe, O. F., Adeyemo, I. A. and Akinmulewo, K. P. (2022): Application of GIS-based PROMETHEE data mining technique to geoelectrical-derived parameters for aquifer potentiality assessment in a typical hardrock terrain Southwestern Nigeria. *Switzerland AG. Sustainable Water Resources Management*, 1-23. DOI.org/10.1007/s40899-022-00616-1.

Najjaran, H., Khajehpour, M., Sharifi, M. and Aalami, M. (2004): Predicting corrosion rate of cast/ductile iron pipes in soil using fuzzy logic. *Corrosion Science*, 46(5), 1115-1126.

Palmer, D. A. (1989): Corrosion of metals in soils. *Corrosion*, 45(4), 297-303.

Picozzi, O. E., Lamb, S. E. and Frank A. C. (1993): Evaluation of prediction methods for pile corrosion at the Bufallo skyway, *New York Department of Transportation, Technical Services Division, Albany, New York.*

Rim-rukch, A. (2006): Effect of soil corrosivity on the performance of the cathodic protection systems. International Journal of Electrochemical Science, 1(3), 123 - 131.

Koefeod O. Geosounding principles, 1. (1979): Resistivity sounding measurements. *Elsevier Scientific Publ*. Comp, Amsterdam, p 275.

Zohdy, A. A. R., Eaton, G. P. and Mabey, D. R. (1974): Application of surface geophysics to groundwater investigations, *In Techniques of Water-Resources Investigations of the United States Geological Survey*. Book 2, Chapter D1. 63.